Integrated plasmonic biosensors based on microring resonators

Voronin, K. V.; Stebunov, Yu V.; Arsenin, Aleksey V. ; Volkov, Valentyn S.

Published in:
Journal of Physics: Conference Series (Online)

DOI:
10.1088/1742-6596/1092/1/012162

Publication date:
2018

Document version:
Final published version

Citation for pulished version (APA):
Voronin, K. V., Stebunov, Y. V., Arsenin, A. V., & Volkov, V. S. (2018). Integrated plasmonic biosensors based on microring resonators. *Journal of Physics: Conference Series (Online)*, *1092*, Article 012162.
https://doi.org/10.1088/1742-6596/1092/1/012162

Journal of Physics: Conference Series

Integrated plasmonic biosensors based on microring resonators

To cite this article: K V Voronin *et al* 2018 *J. Phys.: Conf. Ser.* **1092** 012162

METANANO 2018 IOP Publishing
IOP Conf. Series: Journal of Physics: Conf. Series **1092** (2018) 012162 doi:10.1088/1742-6596/1092/1/012162

Integrated plasmonic biosensors based on microring resonators

K V Voronin[1], Y V Stebunov[1,2], A V Arsenin[1,2], V S Volkov[1,2,3]

[1]Moscow Institute of Physics and Technology, Institutskyi 9, 141700 Dolgoprudnyi, Russia
[2]GrapheneTek, 7 Nobel Street, Skolkovo Innovation Center, 143026, Russia
[3]SDU Nano Optics, Mads Clausen Institute, University of Southern Denmark, Campusvej 55, DK-5230, Odense, Denmark

kirill251097voronin@gmail.com

Abstract. We introduce a biosensor scheme comprising a plasmonic microring resonator coupled with a plasmonic bus waveguide. The detection principle is based on the violation of the surface plasmon polariton resonance condition for the microring (which is sensitive to refractive index changes). Analytical calculations and simulations in COMSOL Multiphysics are presented. As a result, we obtained main characteristics of the sensor, such as sensitivity (S=1200 nm) and Q-factor (Q≈100).

1. Introduction

In recent years, researchers have proposed various schemes of optical label-free biosensors, which simultaneously have high sensitivity and small footprint allowing their integration into electronic devices [1]. The operation principle of most optical biosensors is based on the detection of changes in optical properties induced by the adsorption of analyzed substances on the surface of optical structures. An efficient way to track changes in refractive index (RI) is by using photonic microring resonators due to the strong dependence of their optical resonance conditions on the optical properties of surrounding medium [2-6]. The development of plasmonics has significantly influenced the modern biosensing technology, and currently most commercial optical biosensors are based on the surface plasmon resonance excited using Kretschmann configuration [7-11]. In addition, various schemes with plasmon microresonators have also been proposed [12-14].

In this paper we present a compact biosensor based on an integrated plasmonic microring resonator. This scheme has some advantages over SPR biosensors that are commonly used today: it is much more compact and could be integrated into digital devices. The performance of the proposed biosensor is investigated using analytical calculations and numerical simulation in the COMSOL Multiphysics software package, which includes calculations of the biosensing sensitivity and quality factor of the resonator. The coupling between the eigenmodes of the bus waveguide and the resonator leads to the appearance of minima and maxima in transmission spectra. The change in the RI of an external medium causes a wavelength shift of resonant peaks. Despite the fact that plasmonic resonators have much lower quality factor comparing to photonic ones, a sensitivity of about 1.2 μm can be achieved for a biosensor based on a plasmonic microring resonator, whereas the typical sensitivity of biosensors based on photonic resonators does not exceed 0.5 μm. In the present study we use long-range plasmonic waveguides-based metal strips, which allows to increase the quality factor and slightly increase the sensitivity.

2. Optical biosensors design and simulation

The proposed scheme of a plasmonic biosensor comprises a plasmon waveguide based on a metal strip with a thickness of 20 nm and a width of 5 μm, and a microring resonator with a radius of 40 μm and a straight part with a length of 20 nm (figure 1). The plasmonic waveguide is embedded in a homogeneous dielectric medium, while the microring resonator is placed above it. Both the waveguide and microresonator are considered to be made of gold, which is the most widely used plasmonic material [15]. However, the use of thin gold films requires careful determination of their dielectric function [16-17]. In addition, gold can be replaced in plasmonic biosensors by copper, which demonstrates optical properties comparable to gold [15, 18]. A low-k polymer Cytop is chosen as a dielectric because its RI matches with the RI of aqueous solutions. This symmetry is necessary for the excitation of long-range plasmonic modes.

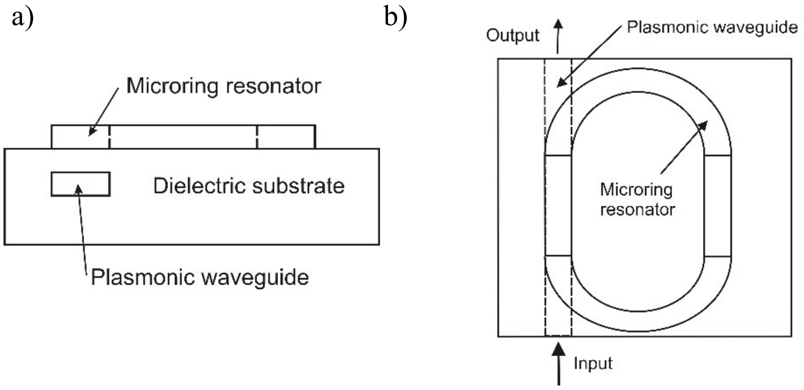

Figure 1. (a) Side and (b) top views of the proposed biosensor scheme comprising the plasmonic waveguide and the microring resonator. The waveguide is embedded in the dielectric substrate and optically coupled with the resonator located above.

A metal film embedded in a uniform dielectric can support two modes of a surface electromagnetic wave: with a symmetric and antisymmetric distributions of the normal component of the electric field. Their propagation constants are calculated from the following transcendental equation.

$$e^{-2k_1 t} = \frac{\frac{k_1}{\varepsilon_1}+\frac{k_2}{\varepsilon_2}\,\frac{k_1}{\varepsilon_1}+\frac{k_3}{\varepsilon_3}}{\frac{k_1}{\varepsilon_1}-\frac{k_2}{\varepsilon_2}\,\frac{k_1}{\varepsilon_1}-\frac{k_3}{\varepsilon_3}} \tag{1}$$

The field distributions for metal films with thicknesses of 10 and 100 nm are shown in Figure 2 (a). In a waveguide of a finite width, these modes are distorted, while demonstrating the similar optical properties. In the following, we consider only a symmetric mode of surface plasmons, since the antisymmetric mode strongly decays in the metal and its practical use is limited. The wave vectors of surface electromagnetic waves propagating in the considered waveguides were found using the simulations performed in the COMSOL Multiphysics software. Another parameter of the system is the coupling constant, which characterizes the transfer of electromagnetic energy between the waveguide and the microresonator. Instead of one long-range (symmetric) mode, the system of two parallel plasmonic waveguides supports two modes with close wave vectors, which have, respectively, symmetric and asymmetric distributions of the resulting electric field (figure 2 (b,c)). The difference between these wave vectors is a coupling constant, which characterizes energy transfer between plasmonic waveguides. Efficient coupling requires that the distance between the waveguides should be no more than the width of the waveguides. The coupling constant is determined by the following formula:

$$C = \frac{(\beta_1 - \beta_2)}{2} \tag{2}$$

Where β1 and β2 are the propagation constants for two eigenmodes existing in the system of two plasmonic waveguides. In the present study, the propagation constants were obtained using simulations in COMSOL.

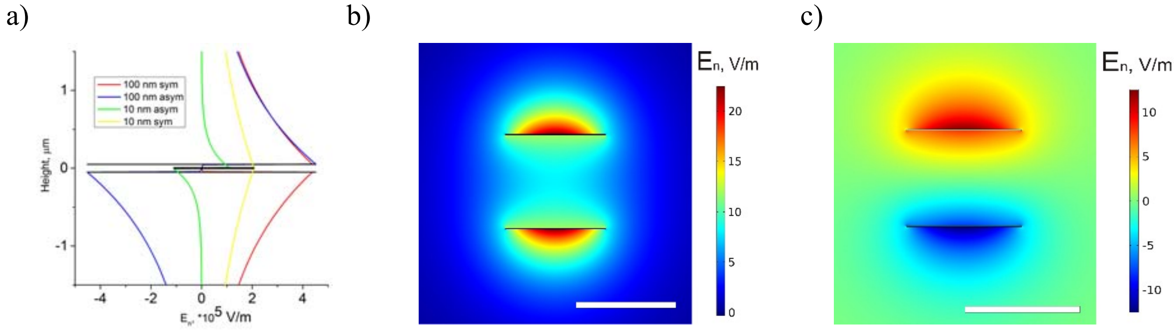

Figure 2. Transverse electric field distributions for symmetric (red line) and asymmetric (blue line) modes of a 100-nm waveguide and for symmetric (green line) and asymmetric (yellow line) modes of a 10-nm waveguide (a). Transverse electric field distributions for two eigenmodes of the system of two plasmonic waveguides (scale bar, 5 µm) (b, c).

3. Results and discussion

The change in the RI can be determined from the wavelength shift of the transmission spectrum. The efficiency of RI sensing is characterized by the sensitivity (S = δλ/δn) and the quality factor (Q) of the microresonator. From simulations, we obtain the wave vector of the plasmonic waveguide, the coupling constant and the attenuation coefficient. Thereafter, we calculate the transmission coefficient for the proposed system using the following equation as in [5]:

$$T = \left| \frac{\cos(CL) - e^{-\gamma l} e^{i\varphi}}{1 - e^{-\gamma l} e^{i\varphi} \cos(\mathrm{CL})} \right|^2 \tag{3}$$

The transmission spectra for different RIs of an analyzed medium are shown in figure 3a. The corresponding sensitivity equals 1.2 µm. The sensitivity to RI changes does not depend on the radius of the resonator and the coupling length but depends mainly on the optical properties of materials and on the width and thickness of the microring resonator (figure 3b).

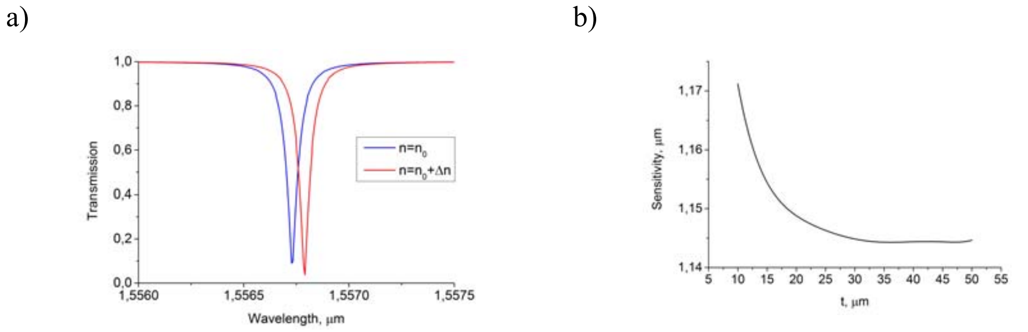

Figure 3. The transmission spectra of the proposed plasmonic biosensor obtained for different RIs of the analyzed solution (a). The sensitivity of the plasmonic biosensor depending on the waveguide thickness (b).

4. Conclusions

We have presented the integrated plasmonic biosensor based on the plasmonic bus waveguide and microring resonator. For considered long-range plasmonic modes, the microring resonator is characterized by the quality factor up to 100, which is higher than for most plasmonic resonators used in biosensing. This resonator is optically coupled to the plasmon waveguide, which is embedded into the dielectric substrate and, therefore, not influenced by the analyzed solution. The obtained sensitivity of 1.2 μm is significantly higher than the corresponding sensitivities of biosensors with photonic and plasmonic resonators, which usually do not exceed 0.3 and 0.6 μm, respectively [19-20]. This result was achieved because of using the metal strip waveguide which is stronger affected by RI changes than dielectric loaded waveguides.

Acknowledgments

This work was supported by the Russian Science Foundation, grant no. 18-19-00684.

References

[1] Roh S, Chung T and Lee B 2011 *Sensors* **11** 1565.
[2] Yang G, White I and Fan X 2008 *Sensors and Actuators* **133** 105.
[3] Xu D, Densmore A, Delâge A, Waldron P, McKinnon R 2008 *Optics express* **16** 15137.
[4] Martin M, Gleeson A, Spaugh B, Tybor F, Gunn W, Hochberg M, Baehr-Jones T, Bailey R and Gunn L 2010 *IEEE J* **16 654**.
[5] Boyd R and Heebner J 2001 *Applied optics* **40** 5742.
[6] Jin L, Li M and He J 2011 *Optics Communications* **284** 156.
[7] Iqbal M, Gleeson M, Spaugh B, Tybor F, Gunn W, Hochberg M, Baehr-Jones T, Bailey R and Gunn L 2010 *J Sel Top Quantum Electron* **16** 654.
[8] Mullett W, Lai E, Jupiter M. Yeung 1998 *Analytical biochemistry* **258** 161.
[9] Gupta G and Kondoh J 2007 *Sens. Actuat. B: Chem* **122** 381.
[10] Stebunov Y V, Aftenieva O A, Arsenin A V, Volkov V S 2015 *ACS Appl. Mater. Interfaces* **7** 21727.
[11] Volkov V S, Stebunov Y V, Yakubovsky D I, Fedyanin D Yu, Arsenin A V 2017 *AIP Conf. Proc.* **1874** 020008.
[12] Homola J, Yee S and Gauglitz G 1999 *Sensors and Actuators* **54** 3.
[13] Debackere P, Taillaert D, De Vos K, Scheerlinck S, Bienstman P and Baets R 2007 *Proc. of SPIE* **6477** 647719.
[14] Lee J, Song J, Sung G, Shin J 2014 *Nano Lett.* **14** 5533.
[15] McPeak K M, Jayanti S V, Kress S J P, Meyer S, Iotti S, Rossinelli A, Norris D J 2015 *ACS Photonics* **2** 326.
[16] Yakubovsky D I, Fedyanin D Yu, Arsenin A V, Volkov V S 2017 *AIP Conf. Proc.* **1874** 040057.
[17] Yakubovsky D I, Arsenin A V, Stebunov Y V, Fedyanin D Y, Volkov V S 2017 *Opt. Express* **25** 25574.
[18] Stebunov Yu V, Yakubovsky D I, Fedyanin D Yu, Arsenin A V, Volkov V S 2018 *Langmuir* (DOI: 10.1021/acs.langmuir.8b00276).
[19] Claes T, Molera J, De Vos K, Schacht E, Baets R and Bienstman P 2009 *IEEE Photonics Journal* **1** 196.
[20] Zhou L, Sun X, Li X and Chen J 2011 *Sensors* **11** 6856.